Wild-type IDH1 affects cell migration by modulating the PI3K/AKT/mTOR pathway in primary glioblastoma cells

XIAOPENG SHEN[1-3*], SHEN WU[1-3*], JINGYI ZHANG[1-3], MENG LI[1-3], FENG XU[1-3], AO WANG[1-3], YANG LEI[4] and GUOPING ZHU[1-3]

[1]Anhui Provincial Key Laboratory of the Conservation and Exploitation of Biological Resources; [2]Anhui Provincial Key Laboratory of Molecular Enzymology and Mechanism of Major Diseases; [3]Key Laboratory of Biomedicine in Gene Diseases and Health of Anhui Higher Education Institutes, College of Life Sciences, Anhui Normal University; [4]Department of Inspection, Wuhu Center for Disease Control and Prevention, Wuhu, Anhui 241000, P.R. China

Received January 13, 2020; Accepted May 18, 2020

DOI: 10.3892/mmr.2020.11250

Abstract. Glioblastoma (GBM) is the most common type of brain cancer and has the highest mortality. Dysregulated expression of wild-type isocitrate dehydrogenase 1 (IDH1) has been demonstrated to promote the progression of primary GBM without accumulating D-2-hydroxyglutarate, which differs from IDH1 mutation-related mechanisms of tumorigenesis. Previous studies have revealed several roles of wild-type IDH1 in primary GBM, involving proliferation and apoptosis. However, the function of IDH1 in cell migration has not been investigated. In the current study, the results of bioinformatics analysis revealed that IDH1 expression was significantly upregulated in patients with primary GBM. Wound healing and Transwell assays demonstrated that IDH1 overexpression promoted cell migration in primary GBM cells and that IDH1 knockdown hindered this process. Furthermore, α-ketoglutarate (α-KG), which is the main product of IDH1-catalyzed reactions, was significantly decreased by IDH1 knockdown and upregulated by IDH1 overexpression. α-KG treatment significantly increased the migration of primary GBM cells. Additionally, RNA sequence analysis of patients with primary GBM reported significant alterations in the expression of phosphoinositide 3-kinase (PI3K)/protein kinase B (AKT)/mammalian target of rapamycin (mTOR) pathway-regulated genes, including Myc, Snail family transcriptional repressor 2 and Twist-related protein 1, which are primarily cell migration regulatory factors. Western blotting revealed that the overexpression or knockdown of IDH1 promoted or inhibited the PI3K/AKT/mTOR pathway, respectively. α-KG treatment of primary GBM cells also promoted the PI3K/AKT/mTOR pathway. Furthermore, IDH1-overexpressing and α-KG-treated U87 cells were incubated with rapamycin, an mTOR-specific inhibitor, and the results revealed that rapamycin treatment reversed the increased cell migration caused by IDH1 overexpression and α-KG treatment. The results indicated that IDH1 regulated the migration of primary GBM cells by altering α-KG levels and that the function of the IDH1/α-KG axis may rely on PI3K/AKT/mTOR pathway regulation.

Correspondence to: Dr Xiaopeng Shen or Dr Guoping Zhu, Key Laboratory of Biomedicine in Gene Diseases and Health of Anhui Higher Education Institutes, College of Life Sciences, Anhui Normal University, 1 East Beijing Road, Wuhu, Anhui 241000, P.R. China
E-mail: shenxiaopeng_cn@ahnu.edu.cn
E-mail: gpz2012@ahnu.edu.cn

*Contributed equally

Key words: primary glioblastoma, isocitrate dehydrogenase 1, α-ketoglutarate, cell migration, phosphoinositide 3-kiase/protein kinase B/mammalian target of rapamycin pathway

Introduction

Glioma is a type of cancer that originates from glial cells in the brain and spinal cord (1). Among gliomas, glioblastoma (GBM) is the most prevalent and has the highest mortality, with a median survival time of <15 months (2) and a 5% 5-year survival rate post-diagnosis worldwide, according to clinical data collected before 2015 (3). Previous studies have focused on the metabolic changes of GBM (4-8). Isocitrate dehydrogenases (IDHs) are a group of enzymes that catalyze isocitrate oxidative decarboxylation to produce α-ketoglutarate (α-KG) and CO_2, that have been reported to exhibit altered activities in GBM due to site mutagenesis and expression level changes (4). The IDHs involved in isocitrate oxidative decarboxylation are crucial for providing metabolic substrates and energy, and regulating the cellular redox status (5-7). Furthermore, α-KG generated from isocitrate oxidative decarboxylation is essential for the α-KG-dependent function of dioxygenase, which is important for DNA and histone demethylation and DNA repair (8).

Previous studies have revealed that the dysregulation of isocitrate dehydrogenase 1 (IDH1) activity, which is caused by site mutations and expression changes, contributed to the occurrence and progression of Ollier disease and Maffucci syndrome (9,10), spondyloenchondromatosis with D-2-hydroxyglutaric aciduria (11), glioblastoma (12-15), acute

myeloid leukemia (16) and early skin tumorigenesis (17), amongst others. Among IDH1 mutations, arginine to histidine substitution at the 132th codon (R132H) is the most prevalent (13). The IDH1 R132H mutant facilitates the reduction of α-KG to D-2-hydroxyglutarate (D-2HG) using NADPH, resulting in a decrease in NADPH and α-KG, and an accumulation of D-2HG (18,19). These alterations lead to extensive epigenetic modification changes, metabolic imbalance, dysregulation of reactive oxygen species and oncogenic substance accumulation (20,21). IDH1 mutations have primarily been discovered in low-grade glioma (LGG), secondary GBM and acute myeloid leukemia (AML); however, they are rare in primary GBM (15). In addition to IDH1 mutations, aberrant IDH1 expression has been correlated with cancer progression and metastasis and whether IDH1 is upregulated or downregulated varies in different types of cancer (13-15). IDH1 is downregulated in early skin cancer, resulting in a higher vulnerability of skin tumorigenesis to tumor-inducing substances (17). In contrast, IDH1 expression was reported to be elevated in numerous types of cancer. For instance, IDH1 is upregulated in non-small cell lung carcinoma (NSCLC) (22). The knockdown of IDH1 using short hairpin (sh)RNAs impedes the growth and proliferation of NSCLC cells (22). IDH1 is also upregulated in 65% of primary GBM cases (15). The inhibition of IDH1 by shRNAs or chemical molecules hinders the growth of GBM cells and extends the survival of mice with tumor xenografts (15). Despite the established roles of IDH1 in cancer, the function of wild-type IDH1 in primary GBM cell migration remains unclear.

Materials and methods

Cell culture. The human GBM cell line U-87 MG (U87; glioblastoma of unknown origin) was purchased from The Cell Bank of Type Culture Collection of the Chinese Academy of Sciences and was authenticated by Short Tandem Repeat profiling as described previously (23). U87 cells were cultured in DMEM (HyClone; Cytiva) supplemented with 10% FBS (Clark Bioscience), 100 U/ml penicillin and 100 μg/ml streptomycin (Biosharp Life Sciences) at 37˚C in a cell culture incubator (Thermo Forma 4131; Thermo Fisher Scientific, Inc.) with 5% CO_2.

To determine the effect of α-Ketoglutarate (α-KG; Sigma-Aldrich; Merck KGaA) on cell migration, U87 cells were treated with 1 or 2.5 mM α-KG supplemented-medium during culture at 37˚C for 24 h. To investigate the effect of the IDH1/α-KG axis on the PI3K/AKT/mTOR signaling pathway, rapamycin (MedChemExpress), an mTOR-specific inhibitor, was used to treat wild-type or IDH1-overexpressing U87 cell cultures at 37˚C for 24 h to block the PI3K/AKT/mTOR signaling pathway. Mock control-treated cells [treated with DMSO (1:200)] were used as controls.

Plasmids and cell transfection. IDH1 overexpression plasmids (pcDNA3-cMyc-IDH1) were generated by inserting IDH1 coding gene fragments into pcDNA3 vectors (Invitrogen; Thermo Fisher Scientific, Inc.). The IDH1 coding gene fragment was amplified from the human cDNA library, which was produced by the reverse transcription of total RNA extracted from 293T cells, using the following primer pairs: Forward (containing the *Bam*HI enzyme site and the cMyc tag sequence), 5'-CCGGATCCGCCACCATGGAGCAGAAGC TGATCTCAGAGGAGGACCTGATGTCCAAAAAAATCA GTGGCG-3' and reverse (containing the *Eco*RI enzyme site), 5'-CGCGAATTCTTAAAGTTTGGCCTGAGCTAGT-3'. The amplified fragment was then ligated into the pcDNA3 vector at the *Bam*HI and *Eco*RI sites. pcDNA3-cMyc-IDH1 plasmids were sequenced to confirm its validity using T7 and SP6 general sequencing primers at General Biosystems, Inc. The pcDNA3 empty vector was used as a control. IDH1 overexpression (OE; IDH1-OE) and control (Ctrl) cell lines were constructed by stably transfecting U87 cells with IDH1 overexpression plasmids (pcDNA3-cMyc-IDH1) and empty vectors (pCDNA3), respectively. IDH1 overexpression was verified by western blotting with antibodies against the cMyc tag and IDH1.

A total of 2 IDH1 shRNA plasmids (shIDH1-1 and shIDH1-2) were produced by inserting shRNA sequences designed against IDH1 into a pLL4.0 vector, which was produced by replacing the GFP expression cassette of the pLL3.7 vector (cat. no. 11795; Addgene, Inc.) with a Neomycin expression cassette. The shRNA sequences were placed downstream of the U6 promoter in the pLL4.0 vector. The shRNAs were designed using the siRNA at WHITEHEAD website (http://jura.wi.mit.edu/bioc/siRNAext) and were synthesized at General Biosystems, Inc. The sense and antisense strands were annealed into double-stranded DNA fragments, which were subsequently phosphorylated. The phosphorylated shRNA fragments were ligated into the pLL4.0 vector at the *Hpa*I and *Xho*I sites. The shRNA plasmids were sequenced to confirm their validity. Scramble shRNA (shScramble) was used as a control. The sequences of the shRNA sense and antisense strands are listed in Table SI.

The plasmid transfections were performed using 1.5 μg plasmid/well and Lipofectamine® 2000 (Invitrogen; Thermo Fisher Scientific, Inc.), according to the manufacturer's protocol, upon the cells reaching 70-90% confluence ($8.0x10^5$ cells/well). Following transfection at 37˚C for 24 h, the culture medium was changed and selection was performed beginning at 48 h post-transfection to generate stable cell lines; 400 μg/ml geneticin (Sigma-Aldrich; Merck KGaA) or 1 μg/ml puromycin (Sangon Biotech Co., Ltd.) was added to the culture medium of cells transfected with the pCDNA3- or pLL4.0-based plasmid.

Western blotting. U87 cell lysates were extracted using Cell Lysis Buffer (Beyotime Institute of Biotechnology) supplemented with protease inhibitors (cOmplete, Mini, EDTA-free Protease Inhibitor Cocktail; Roche Diagnostics), according to the manufacturer's protocol. Protein concentrations were measured using the BCA protein assay kit (Biosharp Life Sciences), according to the manufacturer's protocol, and were adjusted to the same concentration in each set of experiments. Protein samples (4 μg/lane) were subjected to electrophoresis on 10% SDS-PAGE gels and then transferred onto PVDF membranes. The membranes were blocked with 5% bovine serum albumin (Sigma-Aldrich; Merck KGaA) at room temperature for 1 h and incubated with primary antibodies overnight at 4˚C. The membranes were then incubated with horseradish peroxidase (HRP)-conjugated secondary

antibodies at room temperature for 1.5 h and reacted with chemiluminescent substrates (Biosharp Life Sciences). The signals were captured by the Tanon 5200 Imaging system (Tanon 5200; Tanon Science and Technology Co., Ltd.) and the expression levels were analyzed using ImageJ 1.52a software (National Institutes of Health). The antibodies and their dilutions were as follows: cMyc (1:1,000; Thermo Fisher Scientific, Inc.; cat. no. A21280), IDH1 (1:1,000; Hangzhou HuaAn Biotechnology Co., Ltd.; cat. no. EM40705), GAPDH (1:2,000; Biosharp Life Sciences; cat. no. BL006B), phosphorylated (p)-AKT1 (Ser473; 1:1,000; Invitrogen; Thermo Fisher Scientific, Inc.; cat. no. MA120325), AKT (1:1,000; Invitrogen; Thermo Fisher Scientific, Inc.; cat. no. 44609G), mTOR (1:1,000; Cell Signaling Technology, Inc.; cat. no. 2983), p-mTOR (Ser2448; 1:1,000; Cell Signaling Technology, Inc.; cat. no. 9205), goat anti-mouse HRP-conjugated immunoglobulin (Ig) G (1:2,000; Biosharp Life Sciences; cat. no. BL001A) and donkey anti-rabbit HRP-conjugated IgG (1:2,000; Invitrogen; Thermo Fisher Scientific, Inc.; cat. no. 31458).

Total RNA extraction and reverse transcription-quantitative PCR (RT-qPCR). Total RNA was extracted from cells using the Total RNA Isolation reagent (Biosharp Life Sciences). Reverse transcription was performed using the FastKing RT kit (Tiangen Biotech Co., Ltd.), according to the manufacturer's protocol, and qPCR was performed using the Powerup SYBR Master mix (Applied Biosystems; Thermo Fisher Scientific, Inc.), according to the manufacturer's protocol, on an RT-qPCR machine (Bio-Rad CFX96 Touch; Bio-Rad Laboratories, Inc.). The following thermocycling conditions were used for the qPCR: Pre-culture at 50˚C for 120 sec; initial denaturation at 95˚C for 120 sec; 40 cycles of annellation at 95˚C for 15 sec and elongation at 60˚C for 60 sec; and a default dissociation step of 95˚C for 15 sec and then heated from 60-95˚C in incremental steps of 0.2˚C for 15 sec. GAPDH served as an internal control. Gene expression levels were quantified using the $2^{-\Delta\Delta Cq}$ method (24). The primers used for RT-qPCR (IDH1 and GAPDH) are listed in Table SI.

Transwell migration assay. Transwell migration assays were performed as previously reported (25). Transwell inserts with 8.0-μm pore polycarbonate membranes (Corning Inc.) and 24-well plates were utilized. U87 cells were initially seeded at $2.5x10^4$ cells/well in a 100 μl serum-free DMEM, supplemented with 100 U/ml penicillin and 100 μg/ml streptomycin, in the upper chamber. DMEM supplemented with 10% FBS, 100 U/ml penicillin and 100 μg/ml streptomycin was plated into the lower chambers. Following incubation for 20 h at 37˚C in a cell culture incubator with 5% CO_2, the migratory cells were fixed with 4% paraformaldehyde at room temperature for 10 min and then 100% methanol for 10 min at room temperature. Next, the cells were stained with 0.05% crystal violet for 30 min at room temperature. Images were captured using the bright field channel of an Olympus IX71 fluorescence microscope (magnification, x100; Olympus Corporation).

Cell wound healing assay. U87 cells were seeded in 6-well plates at a seeding density of $6x10^5$ cells/well and cultured overnight at 37˚C in a cell culture incubator with 5% CO_2. Wounds were generated by scratching cells with 0-200 μl pipette tips. Following scratching, cells were briefly washed three times with PBS and cultured in DMEM for 48 h. The cells were harvested at 0 and 48 h post-scratch. The cells were washed twice with cold PBS and fixed with chilled methanol for 10 min on ice. Cells were incubated with a staining solution that contained 0.05% crystal violet and 25% methanol for 20 min at room temperature and washed with distilled water. Images were captured with the bright field channel of an Olympus IX71 fluorescence microscope (magnification, x40; Olympus Corporation). The width of the wounds was measured by Canvas X software (version 19; Canvas GFX) and the migratory distances were calculated using the following equation: Scratch width at 0 h-scratch width at 48 h. All migratory distances were normalized to the migratory distances of the control groups at 0 h.

α-KG measurement. α-KG levels in U87 cells were measured using the a-Ketoglutarate Colorimetric/Fluorometric Assay kit (BioVision, Inc.) according to the manufacturer's protocol. The values were determined by measuring absorbance at 570 nm using a TECAN Microplate Reader (Tecan Group, Ltd.).

TCGA data analysis. TCGA data analysis was performed using the UALCAN website (ualcan.path.uab.edu/index.html) (26). GBM samples were selected for analysis; the analysis included 156 primary GBM samples and 5 normal samples. The transcript per million (TPM) of IDH1, AKT, PTEN, CDK2, Myc, MDM2, SNAIL2, N-cadherin, Vimentin, TWIST1, ZEB1 and RAC1 in the above samples were analyzed using the UALCAN website and plotted as boxplots.

Statistical analysis. Experiments were performed in triplicate. All data were normalized to the controls and presented as the mean ± standard deviation, unless otherwise stated. Student's t-tests were used for two-group comparisons and one-way ANOVA, followed by post-hoc Tukey tests, was used for multiple-group comparisons. $P<0.05$ was considered to indicate a statistically significant difference. Significant differences in the statistical analyses are labeled as '*' in all the figures. All statistical analyses were performed using GraphPad Prism software (version 8; GraphPad Software, Inc.).

Results

Downregulation of IDH1 inhibits primary GBM cell migration. Previously, numerous studies have revealed that IDH1 site mutations, particularly the IDH1 R132H mutation, promoted tumorigenesis (13,18-21). However, in primary GBM, IDH1 mutations were not the main cancer-causing factor (15). The analysis of TCGA data demonstrated a significant increase in IDH1 expression in samples from patients with primary GBM compared with adjacent normal samples (Fig. 1A). IDH1 knockdown and scramble control cell lines were constructed by stably transfecting U87 cells with two IDH1 shRNA expression plasmids (shIDH1-1 or shIDH1-2) or shScramble expression plasmids, respectively. IDH1 knockdown was verified by western blotting (Fig. 1B and C) and RT-qPCR (Fig. S1A). Wound healing assays were performed on IDH1 knockdown and scramble shRNA control cells. At 48 h post-scratch, shIDH1-1 and shIDH1-2 groups demonstrated

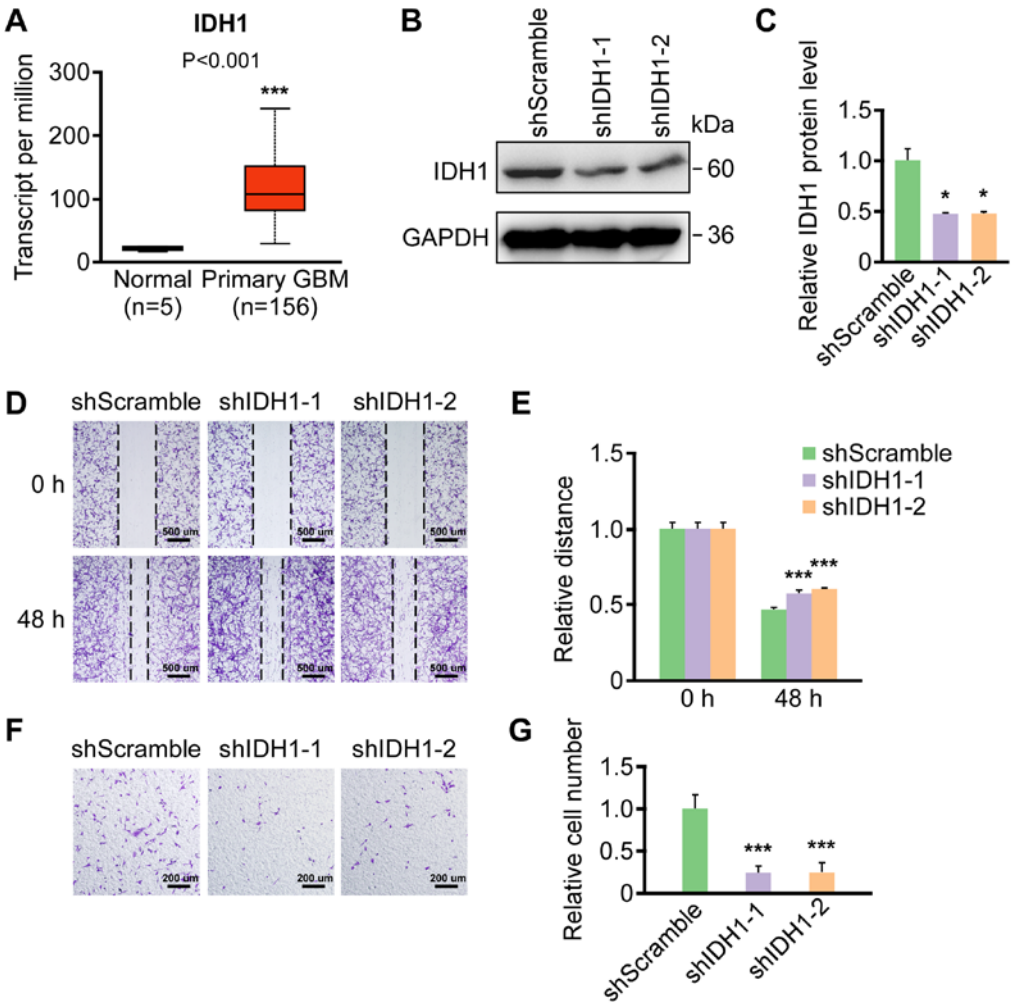

Figure 1. Downregulation of IDH1 inhibited primary GBM cell migration. (A) IDH1 mRNA expression in primary GBM and adjacent normal tissues from The Cancer Genome Atlas is presented. (B) IDH1 knockdown was verified by western blotting. (C) Semi-quantification of the protein expression levels from part (B). (D) IDH1 knockdown repressed the migration of U87 cells as demonstrated by wound healing assays. (E) Semi-quantification of relative migratory distances in part (D). (F) IDH1 knockdown repressed the migration of U87 cells as evidenced by Transwell migration assays. (G) Semi-quantification of relative cell numbers in part (F). *P<0.05; ***P<0.001 vs. shScramble. IDH1, isocitrate dehydrogenase 1; GBM, glioblastoma; shRNA, short hairpin RNA; shScramble, scramble shRNA; shIDH-1/2, IDH1 shRNA plasmids ½.

relatively delayed migration compared with the scramble shRNA group (Fig. 1D and E). Additionally, Transwell migration assays were performed with the same cell lines, the results of which demonstrated that IDH1 knockdown had fewer cells that successfully migrated through the membrane of the Transwell inserts (Fig. 1F and G). In summary, the results indicated that IDH1 downregulation repressed the migration of primary GBM cells.

Upregulation of IDH1 promotes primary GBM cell migration. As the downregulation of IDH1 repressed primary GBM cell migration, the effect of ectopic IDH1 expression on primary GBM cell migration was investigated. The results revealed that cMyc was strongly expressed in the IDH1-OE group; however, it was not detected in the Ctrl group (Fig. 2A). Furthermore, IDH1 expression was significantly increased in the IDH1-OE group compared with the Ctrl group (Fig. 2B). Similarly, IDH1 mRNA levels were increased in the IDH1-OE group, as indicated by RT-qPCR (Fig. S1B). IDH1 expression did not increase markedly, which may be due to IDH1 being endogenously abundant in U87 cells (15). A wound healing assay was then performed on IDH1-OE and control cell lines. Significantly faster migration was observed in the IDH1-OE group (Fig. 2C and D). The results of the Transwell migration assays also demonstrated that IDH1 overexpression promoted U87 cell migration (Fig. 2E and F). In conclusion, IDH1 overexpression facilitated the migration of primary GBM cells.

IDH1 regulates primary GBM cell migration by affecting α-KG levels. Since IDH1 catalyzes the conversion of isocitrate to α-KG and CO_2, whether α-KG levels in primary GBM cells were associated with IDH1 expression was examined. α-KG levels were significantly downregulated in the IDH1 knockdown groups (Fig. 2G) and significantly upregulated when IDH1 was overexpressed (Fig. 2H). Whether α-KG levels affected primary GBM cell migration was then investigated. U87 cells were treated with 1 and 2.5 mM α-KG in the medium during culture. The migration of the U87 cells was promoted by the addition of α-KG in a dose-dependent manner in the wound healing and Transwell assays (Fig. 2I-L). These results indicated that α-KG levels may mediate the changes in migration in primary GBM cells caused by IDH1 level alterations.

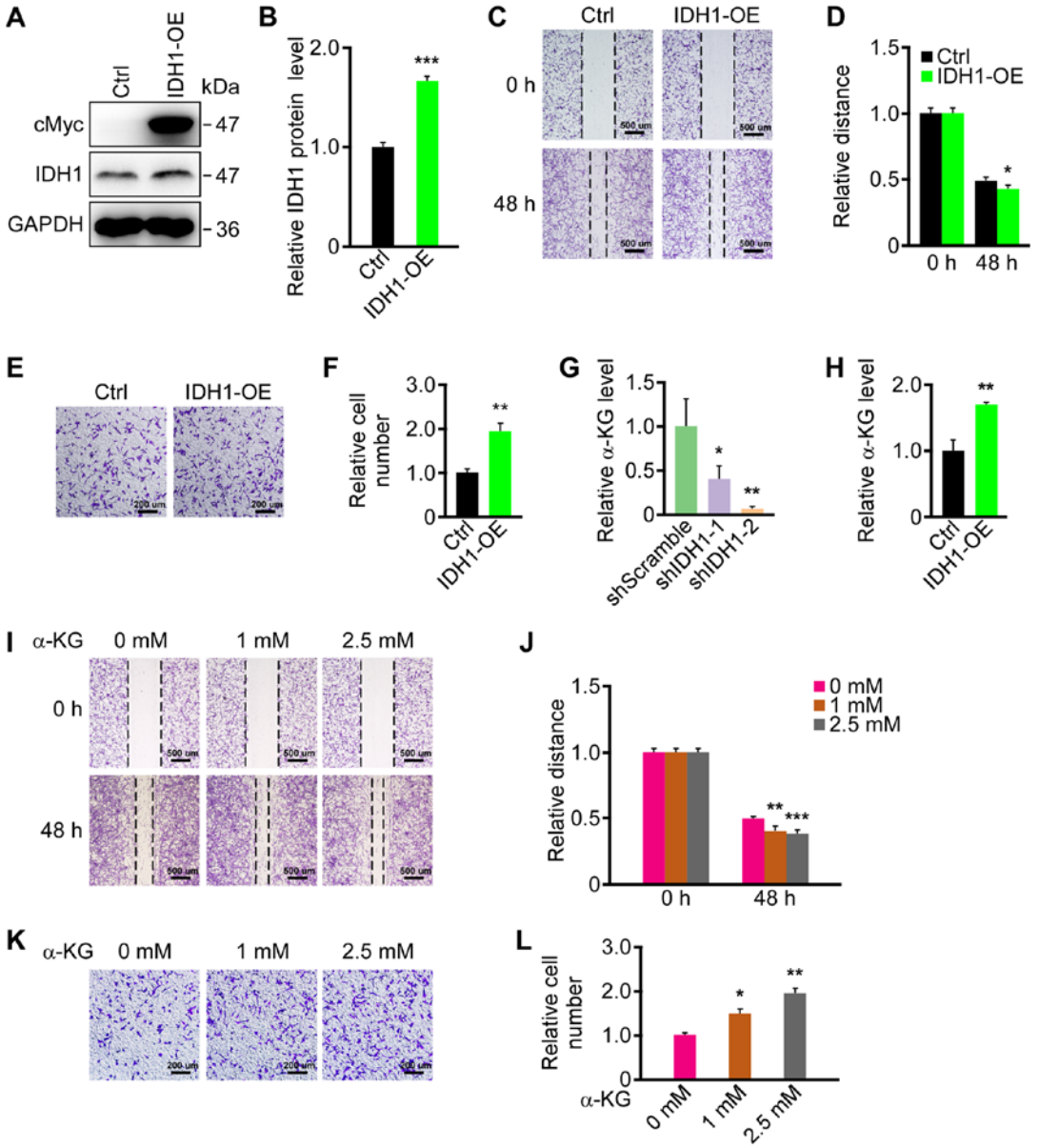

Figure 2. IDH1 overexpression and α-KG treatment promoted primary GBM cell migration. (A) IDH1 overexpression was verified by western blotting. (B) Semi-quantification of expression levels from part (A). (C) IDH1 overexpression promoted the migration of U87 cells as demonstrated by wound healing assays. (D) Semi-quantification of the relative migratory distances in part (C). (E) IDH1 overexpression promoted the migration of U87 cells as revealed by Transwell migration assays. (F) Semi-quantification of relative cell numbers in part (E). (G) α-KG was downregulated by IDH1 knockdown in U87 cells. (H) α-KG was upregulated by IDH1 overexpression in U87 cells. (I) α-KG promoted the migration of U87 cells in wound-healing assays in a dose-dependent manner. (J) Semi-quantification of relative migratory distances in part (I). (K) α-KG promoted the migration of U87 cells in a dose-dependent manner as demonstrated by Transwell migration assays. α-KG treatment lasted for 24 h. (L) Semi-quantification of relative cell numbers in part (K). *P<0.05, **P<0.01, ***P<0.001 vs. shScramble/Ctrl/0 mM. IDH1, isocitrate dehydrogenase 1; α-KG, α-ketoglutarate; GBM, glioblastoma; Ctrl, control; IDH1-OE, IDHI1 overexpression cell line; shScramble, scramble shRNA; shIDH-1/2, IDH1 shRNA plasmids 1/2; shRNA, short hairpin RNA.

PI3K/AKT/mTOR pathway activity is enhanced in primary GBM. Primary GBM is a type of cancer with the highest mortality partly due to its relatively high migration rate (27,28). TCGA database analysis revealed that PI3K/AKT/mTOR pathway activity was significantly increased in primary GBM. AKT and phosphatase and tensin homolog, which are key components of the PI3K/AKT/mTOR pathway, were significantly upregulated and downregulated in primary GBM, respectively (Fig. S2A). The expression of the genes downstream of the PI3K/AKT/mTOR pathway and whose expression is regulated by the pathway was then examined. Cyclin-dependent kinase 2, Myc and mouse double minute 2 homolog were significantly upregulated in primary GBM, which are proteins that promote the cell cycle and repress apoptosis (Fig. S2B) (29). Snail family transcriptional repressor 2, N-cadherin and vimentin were also significantly upregulated, which facilitate the epithelial-mesenchymal transition (EMT) process (Fig. S2C). Additionally, twist-related protein 1, zinc finger E-box-binding homeobox 1 and Ras-related C3 botulin toxin substrate 1 were upregulated, which are proteins that enhance cell migration and metastasis (Fig. S2D) (29-31). The results indicated that the PI3K/AKT/mTOR pathway was hyperactivated in primary GBM, which is associated with the cell cycle, apoptosis, EMT, cell migration and metastasis processes (32-36).

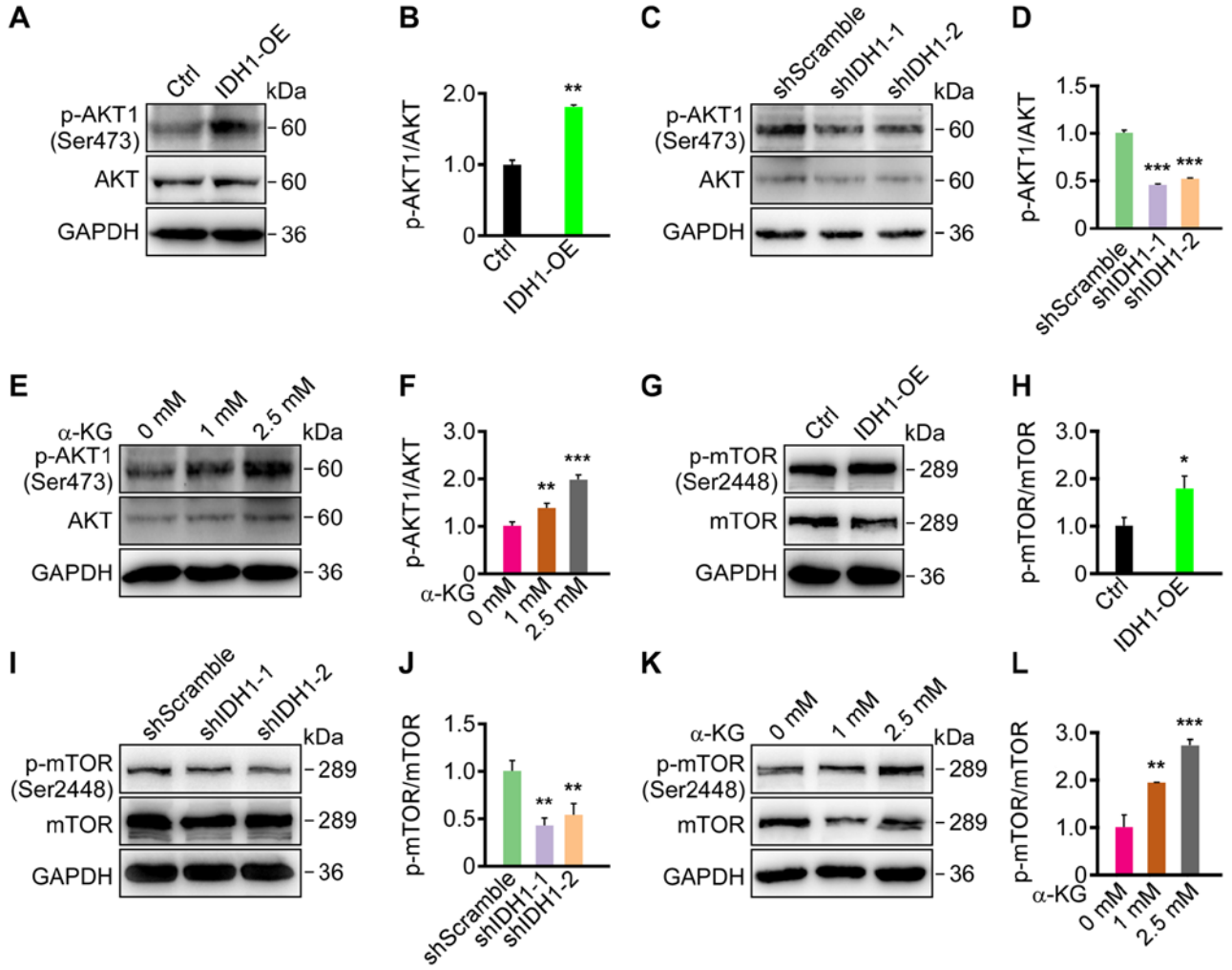

Figure 3. Phosphoinositide 3-kinase/AKT/mTOR pathway activity was altered by changes in the levels of IDH1 and α-KG in primary GBM cells. (A) p-AKT (Ser473) was promoted by IDH1 overexpression in U87 cells. (B) Semi-quantification of the expression levels from part (A). (C) p-AKT (Ser473) was decreased by IDH1 knockdown in U87 cells. (D) Semi-quantification of expression levels from part (C). (E) p-AKT (Ser473) was promoted by α-KG treatment in a dose-dependent manner in U87 cells. (F) Semi-quantification of the expression levels from part (E). (G) p-mTOR (Ser2448) was promoted by IDH1 overexpression in U87 cells. (H) Semi-quantification of the expression levels from (G). (I) p-mTOR (Ser2448) was repressed by IDH1 knockdown in U87 cells. (J) Semi-quantification of the expression levels from part (I). (K) p-mTOR (Ser2448) was promoted by α-KG treatment in a dose-dependent manner in U87 cells. α-KG treatment lasted for 24 h. (L) Semi-quantification of the expression levels from part (K). *P<0.05, **P<0.01, ***P<0.001 vs. shScramble/Ctrl/0 mM. p, phosphorylated; AKT, protein kinase B; IDH1, isocitrate dehydrogenase 1; α-KG, α-ketoglutarate; GBM, glioblastoma; Ser, serine; Ctrl, control; IDH1-OE, IDHI1 overexpression cell line; shRNA, short hairpin RNA; shScramble, scramble shRNA; shIDH-1/2, IDH1 shRNA plasmids 1/2.

PI3K/AKT/mTOR pathway activity is altered by changes in IDH1 and α-KG levels in primary GBM cells. As PI3K/AKT/mTOR pathway activity was increased in primary GBM, whether IDH1 and α-KG expression affected the PI3K/AKT/mTOR pathway was investigated. The results of western blotting revealed that IDH1 knockdown and overexpression resulted in the downregulation and upregulation of p-AKT (Ser473) and the p-mTOR (Ser2448), respectively, in primary GBM cells (Fig. 3A-D and G-J). By treating primary GBM cells with 1 and 2.5 mM α-KG, p-AKT (Ser473) and p-mTOR (Ser2448) were significantly upregulated in a dose-dependent manner (Fig. 3E, F and K, L). The results indicated that IDH1 and α-KG levels regulated PI3K/AKT/mTOR pathway activity in primary GBM cells.

The IDH1/α-KG axis regulates primary GBM cell migration through the PI3K/AKT/mTOR pathway. As PI3K/AKT/mTOR pathway activity was regulated by changes in the IDH1 and α-KG levels, whether IDH1/α-KG regulated primary GBM cell migration by modulating the PI3K/AKT/mTOR pathway was examined. Wild-type U87 cells were treated with rapamycin, which is an mTOR-specific inhibitor, to block the PI3K/AKT/mTOR pathway. Mock control-treated cells were used as controls. Western blotting results reported that p-mTOR (Ser2448) was significantly inhibited by rapamycin treatment compared with controls (Fig. S3A and B). Additionally, rapamycin treated U87 cells exhibited significantly delayed cell migration compared with controls, indicating that blocking the PI3K/AKT/mTOR pathway led to the repression of cell migration (Fig. S3C and D). Furthermore, IDH1-overexpressing U87 cells and α-KG-treated U87 cells were treated with rapamycin. Western blotting results demonstrated that p-mTOR (Ser2448) was repressed by rapamycin in both treatment groups (Fig. 4A-D). The increased cell migration caused by IDH1 overexpression and α-KG supplementation were also reversed following rapamycin treatment (Fig. 4E-H). The

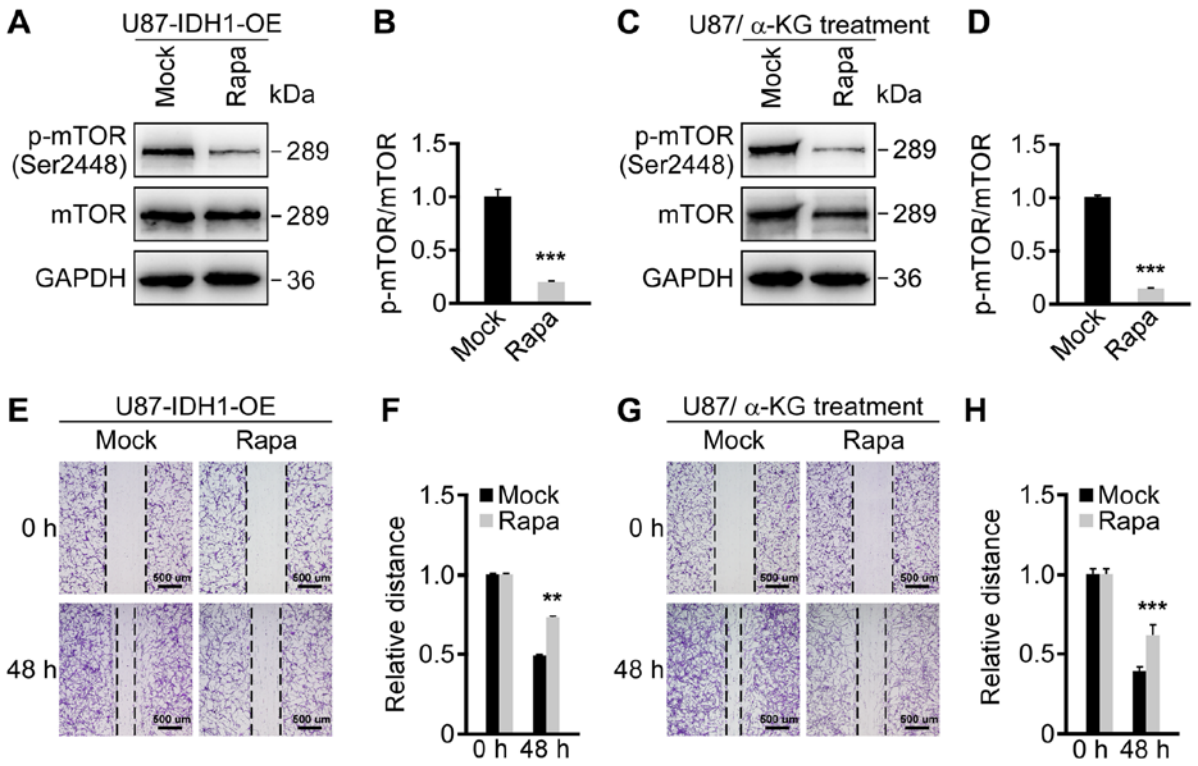

Figure 4. IDH1/α-KG axis regulated primary GBM cell migration through the Phosphoinositide 3-kinase/protein kinase B/mTOR pathway. (A) p-mTOR (Ser2448) was repressed by rapamycin in IDH1-overexpressing U87 cells. (B) Semi-quantification of expression levels from part (A). (C) p-mTOR (Ser2448) was repressed by rapamycin in α-KG-treated U87 cells. (D) Semi-quantification of the expression levels from part (C). (E) Rapamycin treatment reversed the IDH1 overexpression-induced enhancement of migration in U87 cells. (F) Semi-quantification of the relative migratory distances in part (E). (G) Rapamycin treatment reversed the α-KG supplementation-induced enhancement of migration in U87 cells. α-KG and rapamycin treatments lasted for 24 h. (H) Semi-quantification of relative migratory distances in part (G). **P<0.01, ***P<0.001 vs. Mock. IDH1, isocitrate dehydrogenase 1; α-KG, α-ketoglutarate; GBM, glioblastoma; mTOR, mammalian target of rapamycin; p-, phosphorylated; IDH1-OE, IDHI1 overexpression cell line; Rapa, rapamycin; Mock, controls.

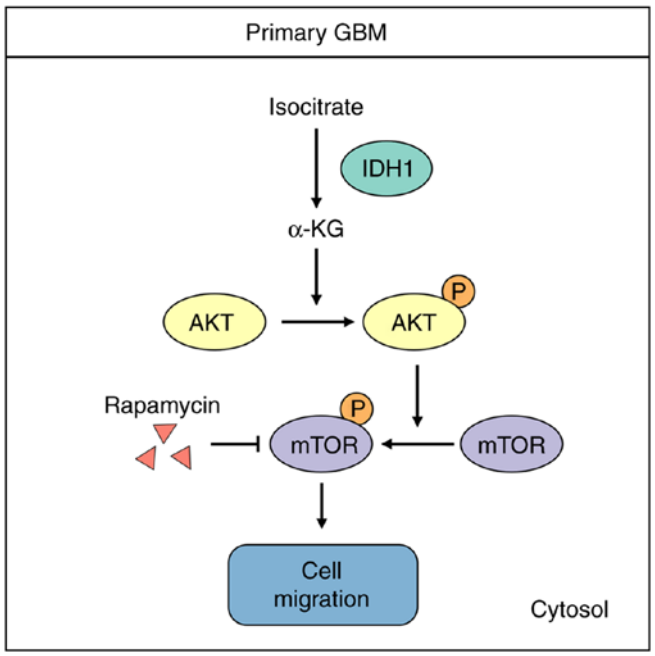

Figure 5. A working model of wild-type IDH1 in primary GBM cells. IDH1 is the enzyme that catalyzes α-KG production from isocitrate. Wild-type IDH1 promotes the activation of the PI3K/AKT/mTOR pathway by affecting α-KG levels. IDH1 and α-KG may regulate primary GBM cell migration by modulating the PI3K/AKT/mTOR pathway. IDH1, isocitrate dehydrogenase 1; GBM, glioblastoma; α-KG, α-ketoglutarate; PI3K, phosphoinositide 3-kinase; AKT, protein kinase B; mTOR, mammalian target of rapamycin; P, phosphorylated.

results indicated that the IDH1/α-KG axis regulated primary GBM cell migration by modulating the PI3K/AKT/mTOR pathway (Fig. 5).

Discussion

IDH1 is an important enzyme in cell metabolism that catalyzes the oxidative decarboxylation of isocitrate to produce α-KG, NADPH and CO_2 (37). The roles of site-mutated IDH1 in tumorigenesis are well established (13,18-21); however, the function of wild-type IDH1 in cancer has not been studied extensively. Clinical data has demonstrated that site-mutated IDH1 was mainly detected in LGG, secondary GBM and AML; however, it was observed in only 5% of patients with primary GBM (15). According to TCGA database, IDH1 expression was significantly upregulated in primary GBM, which indicated that alterations in wild-type IDH1 levels may contribute to primary GBM tumorigenesis. This result was consistent with that of a previous study, where wild-type IDH1 was upregulated in primary GBM, instead of being mutated (15). Thus, whether upregulated IDH1 expression was crucial to primary GBM progression was subsequently investigated. Calvert *et al* (15) reported that IDH1 suppression via shRNA or specific inhibitors inhibited primary GBM growth and facilitated cellular differentiation. However, the role of IDH1 in primary GBM cell migration remains elusive. Considering that primary GBM is a type of cancer that exhibits

relatively high migratory abilities (27,28), excess IDH1 was hypothesized to contribute to primary GBM migration. The current study discovered that IDH1 knockdown or overexpression led to repressed or improved cell migration, respectively.

α-KG is primarily produced by IDH1 via oxidative decarboxylation (38,39). Therefore, whether α-KG mediated the effect of wild-type IDH1 on primary GBM cell migration was investigated. Cellular α-KG levels were positively associated with changes in IDH1 levels. By treating U87 cells with different concentrations of α-KG, dose-dependent increases in the migration rates of primary GBM cells were observed. However, to the best of our knowledge, there is no applicable method to directly reduce α-KG levels in live cells, which impeded the current study to examine the effect of decreased α-KG on cell migration. The most common way to reduce α-KG levels in live cells is to repress enzymes that catalyze the production of α-KG, such as IDH1. Therefore, the current study investigated the effect of IDH1 knockdown and the results matched expectations. Thus, the changes in the migration of primary GBM cells mediated by changes in IDH1 levels may occur by altering α-KG levels.

The PI3K/AKT/mTOR pathway regulates multiple cellular events, including growth, proliferation, motility and survival, which are often dysregulated in cancer (40). Although numerous previous studies (41-43) have reported the effect of the IDH1 R132H mutation on the PI3K/AKT/mTOR pathway, the correlation remains unclear. While IDH1 R132H and D-2HG were discovered to inhibit the PI3K/AKT/mTOR pathway in human glioma samples (41), another previous study reported that IDH1 R132H and 2-HG promoted the PI3K/AKT/mTOR pathway, resulting in upregulated glioma migration (44,45). Despite previous reports on mutated IDH1, the function of wild-type IDH1 and α-KG levels on the PI3K/AKT/mTOR pathway remain unclear. The current study revealed that PI3K/AKT/mTOR pathway activity was enhanced by IDH1 overexpression and α-KG treatment, and repressed by IDH1 knockdown. To further investigate whether the IDH1/α-KG axis regulated primary GBM cell migration by modulating the PI3K/AKT/mTOR pathway, rapamycin treatment combined with IDH1 overexpression or α-KG supplementation was employed. The results demonstrated that the increased cell migration of primary GBM cells was reversed, indicating that the IDH1/α-KG axis regulated cell migration in primary GBM cells via the PI3K/AKT/mTOR pathway.

Despite the mechanism revealed in the present study, there are areas of research that require further study. Firstly, as the results of the current study demonstrated that IDH1 may be a potential therapeutic target or diagnostic marker in primary GBM, further *in vivo* investigations are required prior to clinical application. Secondly, although α-KG levels were reported to regulate the PI3K/AKT/mTOR pathway in primary GBM cells, the detailed mechanism of how α-KG affected the PI3K/AKT/mTOR pathway remains, to the best of our knowledge, unknown and should be investigated in future studies.

In conclusion, the current study discovered that the wild-type IDH1/α-KG axis regulated primary GBM cell migration through the PI3K/AKT/mTOR pathway. In contrast to numerous previous reports that focused on the roles of IDH1 mutations in tumorigenesis (13,18-21), the present study was, to the best of our knowledge, the first study on the function of wild-type IDH1 in primary GBM cell migration. Moreover, the results demonstrated that α-KG was the intermediate molecule between IDH1 and the PI3K/AKT/mTOR pathway. This mechanism reported by the current study expanded the understanding of the process of primary GBM tumorigenesis and may be beneficial for therapy against primary GBM.

Acknowledgements

Not applicable.

Funding

The current study was funded by the National Natural Science Foundation of China (grant no. 31701289), Anhui Provincial Natural Science Foundation (grant no. 1808085QH234), Anhui Provincial Funding Scheme to Outstanding Innovative Programs by Returned Scholars (grant no. 2019LCX003), Educational Commission of Anhui Province of China (grant nos. KJ2017A319 and KJ2019A0498), Foundation for High-level Talents in Higher Education of Anhui Province of China [grant no. (2017)51] and the Anhui Normal University (grant no. 2017XJJ38; start-up funds to XS).

Availability of data and materials

The datasets used and/or analyzed during the current study are available from the corresponding author on reasonable request.

Authors' contributions

XS, SW, JZ, ML, FX, AW, YL and GZ collected and analyzed the data. XS and SW conceptualized the current study. AW and YL prepared materials. XS, SW and GZ wrote the original manuscript. XS reviewed and edited the manuscript. XS and GZ supervised the current study. All authors read and approved the final manuscript.

Ethics approval and consent to participate

Not applicable.

Patient consent for publication

Not applicable.

Competing interests

The authors declare that they have no competing interests.

References

1. Mamelak AN and Jacoby DB: Targeted delivery of antitumoral therapy to glioma and other malignancies with synthetic chlorotoxin (TM-601). Expert Opin Drug Deliv 4: 175-186, 2007.
2. Yang K, Niu L, Bai Y and Le W: Glioblastoma: Targeting the autophagy in tumorigenesis. Brain Res Bull 153: 334-340, 2019.
3. Gallego O: Nonsurgical treatment of recurrent glioblastoma. Curr Oncol 22: e273-e281, 2015.
4. Bergaggio E and Piva R: Wild-type IDH enzymes as actionable targets for cancer therapy. Cancers (Basel) 11: 563, 2019.
5. Kirkman HN, Galiano S and Gaetani GF: The function of catalase-bound NADPH. J Biol Chem 262: 660-666, 1987.

6. Itsumi M, Inoue S, Elia AJ, Murakami K, Sasaki M, Lind EF, Brenner D, Harris IS, Chio IIC, Afzal S, *et al*: Idh1 protects murine hepatocytes from endotoxin-induced oxidative stress by regulating the intracellular NADP(+)/NADPH ratio. Cell Death Differ 22: 1837-1845, 2015.
7. Lee SM, Koh HJ, Park DC, Song BJ, Huh TL and Park JW: Cytosolic NADP(+)-dependent isocitrate dehydrogenase status modulates oxidative damage to cells. Free Radic Biol Med 32: 1185-1196, 2002.
8. Gagné LM, Boulay K, Topisirovic I, Huot ME and Mallette FA: Oncogenic activities of IDH1/2 mutations: From epigenetics to cellular signaling. Trends Cell Biol 27: 738-752, 2017.
9. Pansuriya TC, van Eijk R, d'Adamo P, van Ruler M, Kuijjer ML, Oosting J, Cleton-Jansen AM, van Oosterwijk JG, Verbeke SLF, Meijer D, *et al*: Somatic mosaic IDH1 and IDH2 mutations are associated with enchondroma and spindle cell hemangioma in ollier disease and maffucci syndrome. Nat Genet 43: 1256-1261, 2011.
10. Pansuriya TC, Kroon HM and Bovee JV: Enchondromatosis: Insights on the different subtypes. Int J Clin Exp Pathol 3: 557-569, 2010.
11. Struys EA, Salomons GS, Achouri Y, Van Schaftingen E, Grosso S, Craigen WJ, Verhoeven NM and Jakobs C: Mutations in the D-2-hydroxyglutarate dehydrogenase gene cause D-2-hydroxyglutaric aciduria. Am J Hum Genet 76: 358-360, 2005.
12. Parsons DW, Jones S, Zhang X, Lin JCH, Leary RJ, Angenendt P, Mankoo P, Carter H, Siu IM, Gallia GL, *et al*: An integrated genomic analysis of human glioblastoma multiforme. Science 321: 1807-1812, 2008.
13. Yan H, Parsons DW, Jin G, McLendon R, Rasheed BA, Yuan W, Kos I, Haberle IB, Jones S, Riggins GJ, *et al*: IDH1 and IDH2 mutations in gliomas. N Engl J Med 360: 765-773, 2009.
14. Balss J, Meyer J, Mueller W, Korshunov A, Hartmann C and von Deimling A: Analysis of the IDH1 codon 132 mutation in brain tumors. Acta Neuropathol 116: 597-602, 2008.
15. Calvert AE, Chalastanis A, Wu Y, Hurley LA, Kouri FM, Bi Y, Kachman M, May JL, Bartom E, Hua Y, *et al*: Cancer-associated IDH1 promotes growth and resistance to targeted therapies in the absence of mutation. Cell Rep 19: 1858-1873, 2017.
16. Ma QL, Wang JH, Wang YG, Hu C, Mu QT, Yu MX, Wang L, Wang DM, Yang M, Yin XF, *et al*: High IDH1 expression is associated with a poor prognosis in cytogenetically normal acute myeloid leukemia. Int J Cancer 137: 1058-1065, 2015.
17. Robbins D, Wittwer JA, Codarin S, Circu ML, Aw TY, Huang TT, Van Remmen H, Richardson A, Wang DB, Witt SN, *et al*: Isocitrate dehydrogenase 1 is downregulated during early skin tumorigenesis which can be inhibited by overexpression of manganese superoxide dismutase. Cancer Sci 103: 1429-1433, 2012.
18. DiNardo CD, Jabbour E, Ravandi F, Takahashi K, Daver N, Routbort M, Patel KP, Brandt M, Pierce S, Kantarjian H and Manero GG: IDH1 and IDH2 mutations in myelodysplastic syndromes and role in disease progression. Leukemia 30: 980-984, 2016.
19. Dang L, White DW, Gross S, Bennett BD, Bittinger MA, Driggers EM, Fantin VR, Jang HG, Jin S, Keenan MC, *et al*: Cancer-associated IDH1 mutations produce 2-hydroxyglutarate. Nature 462: 739-744, 2009.
20. Lu C, Ward PS, Kapoor GS, Rohle D, Turcan S, Wahab OA, Edwards CR, Khanin R, Figueroa ME, Melnick A, *et al*: IDH mutation impairs histone demethylation and results in a block to cell differentiation. Nature 483: 474-478, 2012.
21. Xu W, Yang H, Liu Y, Yang Y, Wang P, Kim SH, Ito S, Yang C, Wang P, Xiao NT, *et al*: Oncometabolite 2-hydroxyglutarate is a competitive inhibitor of alpha-ketoglutarate-dependent dioxygenases. Cancer Cell 19: 17-30, 2011.
22. Tan F, Jiang Y, Sun N, Chen Z, Lv Y, Shao K, Li N, Qiu B, Gao Y, Li B, *et al*: Identification of isocitrate dehydrogenase 1 as a potential diagnostic and prognostic biomarker for non-small cell lung cancer by proteomic analysis. Mol Cell Proteomics 11: M111 008821, 2012.
23. Reid Y, Storts D, Riss T and Minor L: Authentication of human cell lines by STR DNA profiling analysis. In: Assay Guidance Manual (Internet). Bethesda (MD). Sittampalam GS, Grossman A, Brimacombe K, Arkin M, Auld D, Austin CP, Baell J, Bejcek B, Caaveiro JMM, Chung TDY, *et al* (eds): Eli Lilly & Company and the National Center for Advancing Translational Sciences, 2013. https://www.ncbi.nlm.nih.gov/books/NBK144066/. Accessed May 1, 2013.
24. Livak KJ and Schmittgen TD: Analysis of relative gene expression data using real-time quantitative PCR and the 2(-Delta Delta C(T)) method. Methods 25: 402-408, 2001.
25. van de Merbel AF, van der Horst G, Buijs JT and van der Pluijm G: Protocols for migration and invasion studies in prostate cancer. Methods Mol Biol 1786: 67-79, 2018.
26. Chandrashekar DS, Bashel B, Balasubramanya SAH, Creighton CJ, Rodriguez IP, Chakravarthi BV and Varambally S: UALCAN: A portal for facilitating tumor subgroup gene expression and survival analyses. Neoplasia 19: 649-658, 2017.
27. Holland EC: Gliomagenesis: Genetic alterations and mouse models. Nat Rev Genet 2: 120-129, 2001.
28. Nakada M, Nakada S, Demuth T, Tran NL, Hoelzinger DB and Berens ME: Molecular targets of glioma invasion. Cell Mol Life Sci 64: 458-478, 2007.
29. Ersahin T, Tuncbag N and Cetin-Atalay R: The PI3K/AKT/mTOR interactive pathway. Mol Biosyst 11: 1946-1954, 2015.
30. Lamouille S, Xu J and Derynck R: Molecular mechanisms of epithelial-mesenchymal transition. Nat Rev Mol Cell Biol 15: 178-196, 2014.
31. Gonzalez DM and Medici D: Signaling mechanisms of the epithelial-mesenchymal transition. Sci Signal 7: re8, 2014.
32. Popolo A, Pinto A, Daglia M, Nabavi SF, Farooqi AA and Rastrelli L: Two likely targets for the anti-cancer effect of indole derivatives from cruciferous vegetables: PI3K/Akt/mTOR signalling pathway and the aryl hydrocarbon receptor. Semin Cancer Biol 46: 132-137, 2017.
33. Lee HJ, Venkatarame Gowda Saralamma V, Kim SM, Ha SE, Raha S, Lee WS, Kim EH, Lee SJ, Heo JD and Kim GS: Pectolinarigenin induced cell cycle arrest, autophagy, and apoptosis in gastric cancer cell via PI3K/AKT/mTOR signaling pathway. Nutrients 10: 1043, 2018.
34. Zhang H, Xu HL, Wang YC, Lu ZY, Yu XF and Sui DY: 20(S)-protopanaxadiol-induced apoptosis in MCF-7 breast cancer cell line through the inhibition of PI3K/AKT/mTOR signaling pathway. Int J Mol Sci 19: 1053, 2018.
35. Larue L and Bellacosa A: Epithelial-mesenchymal transition in development and cancer: Role of phosphatidylinositol 3' kinase/AKT pathways. Oncogene 24: 7443-7454, 2005.
36. Vanhaesebroeck B, Guillermet-Guibert J, Graupera M and Bilanges B: The emerging mechanisms of isoform-specific PI3K signalling. Nat Rev Mol Cell Biol 11: 329-341, 2010.
37. Geisbrecht BV and Gould SJ: The human PICD gene encodes a cytoplasmic and peroxisomal NADP(+)-dependent isocitrate dehydrogenase. J Biol Chem 274: 30527-30533, 1999.
38. Dimitrov L, Hong CS, Yang C, Zhuang Z and Heiss JD: New developments in the pathogenesis and therapeutic targeting of the IDH1 mutation in glioma. Int J Med Sci 12: 201-213, 2015.
39. Xu X, Zhao J, Xu Z, Peng B, Huang Q, Arnold E and Ding J: Structures of human cytosolic NADP-dependent isocitrate dehydrogenase reveal a novel self-regulatory mechanism of activity. J Biol Chem 279: 33946-33957, 2004.
40. Janku F, Yap TA and Meric-Bernstam F: Targeting the PI3K pathway in cancer: Are we making headway? Nat Rev Clin Oncol 15: 273-291, 2018.
41. Birner P, Pusch S, Christov C, Mihaylova S, Uzeir KT, Natchev S, Schoppmann SF, Tchorbanov A, Streubel B, Tuettenberg J and Guentchev M: Mutant IDH1 inhibits PI3K/Akt signaling in human glioma. Cancer 120: 2440-2447, 2014.
42. Noushmehr H, Weisenberger DJ, Diefes K, Phillips HS, Pujara K, Berman BP, Pan F, Pelloski CE, Sulman EP, Bhat KP, *et al*: Identification of a CpG island methylator phenotype that defines a distinct subgroup of glioma. Cancer Cell 17: 510-522, 2010.
43. Bralten LB, Kloosterhof NK, Balvers R, Sacchetti A, Lapre L, Lamfers M, Leenstra S, Jonge Hd, Kros JM, Jansen EEW, *et al*: IDH1 R132H decreases proliferation of glioma cell lines in vitro and in vivo. Ann Neurol 69: 455-463, 2011.
44. Zhu H, Zhang Y, Chen J, Qiu J, Huang K, Wu M and Xia C: IDH1 R132H mutation enhances cell migration by activating AKT-mTOR signaling pathway, but sensitizes cells to 5-FU treatment as nadph and gsh are reduced. PLoS One 12: e0169038, 2017.
45. Carbonneau M, Gagné LM, Lalonde ME, Germain MA, Motorina A, Guiot MC, Secco B, Vincent EE, Tumber A, Hulea L, *et al*: The oncometabolite 2-hydroxyglutarate activates the mTOR signalling pathway. Nat Commun 7: 12700, 2016.